Original Article

MOLECULAR METABOLISM

Wolfram syndrome 2 gene (CISD2) deficiency disrupts Ca^{2+}-mediated insulin secretion in β-cells

Zhao-Qing Shen[1,9], Wen-Tai Chiu[2,9], Cheng-Heng Kao[3,9], Yu-Chen Chen[1], Li-Hsien Chen[4], Tsai-Wen Teng[1], Shao-Yu Hsiung[1], Tsai-Yu Tzeng[5], Chien-Yi Tung[5], Chi-Chang Juan[6], Ting-Fen Tsai[1,7,8,*]

ABSTRACT

Objective: Diabetes, characterized by childhood-onset, autoantibody-negativity and insulin-deficiency, is a major manifestation of Wolfram syndrome 2 (WFS2), which is caused by recessive mutations of CISD2. Nevertheless, the mechanism underlying β-cell dysfunction in WFS2 remains elusive. Here we delineate the essential role of CISD2 in β-cells.

Methods: We use β-cell specific Cisd2 knockout (Cisd2KO) mice, a CRISPR-mediated Cisd2KO MIN6 β-cell line and transcriptomic analysis.

Results: Four findings are pinpointed. Firstly, β-cell specific Cisd2KO in mice disrupts systemic glucose homeostasis via impairing β-granules synthesis and insulin secretion; hypertrophy of the β-islets and the presence of a loss of identity that affects certain β-cells. Secondly, Cisd2 deficiency leads to impairment of glucose-induced extracellular Ca^{2+} influx, which compromises Ca^{2+}-mediated insulin secretory signaling, causing mitochondrial dysfunction and, thereby impairing insulin secretion in the MIN6-Cisd2KO β-cells. Thirdly, transcriptomic analysis of β-islets reveals that Cisd2 modulates proteostasis and ER stress, mitochondrial function, insulin secretion and vesicle transport. Finally, the activated state of two potential upstream regulators, Glis3 and Hnf1a, is significantly suppressed under Cisd2 deficiency; notably, their downstream target genes are deeply involved in β-cell function and identity.

Conclusions: These findings provide mechanistic insights and form a basis for developing therapeutics for the effective treatment of diabetes in WFS2 patients.

Keywords CISD2; Wolfram syndrome 2; Diabetes; Ca^{2+} homeostasis; Mitochondrial function

1. INTRODUCTION

Wolfram syndrome (WFS) (MIM 222300) exhibits a highly variable clinical spectrum that includes Diabetes Insipidus, Diabetes Mellitus, Optic Atrophy, and Deafness. These are collectively known as the DIDMOAD syndrome [1]. WFS patients have a form of diabetes that does not fit into currently diagnostic criteria of type 1 or type 2 diabetes. The clinical manifestations of diabetes in WFS patients are characterized by a childhood-onset of diabetes with autoantibody-negativity together with the diabetes being caused by insulin-deficiency with no evidence of insulin resistance. These clinical features thus have the form of an atypical diabetes [2,3]. Several β-cell alterations in atypical diabetes have been characterized, including reduced insulin secretory responses, enhanced endoplasmic reticulum (ER) stress, and increased oxidative stress, as well as senescence and cell death [2,3].

WFS is categorized into two major types. The first type is WFS1 (MIM 606201), which is caused by recessive mutations of WFS1 (Wolframin). This gene encodes a transmembrane protein primarily localized in the ER. The second type is WFS2 (MIM 604928), which is caused by recessive mutations of CDGSH iron-sulfur domain-containing protein 2 (CISD2). Several mutations of the CISD2 gene have been identified in WFS2 patients and mutations affecting the CISD2 protein are associated with dysregulation of Ca^{2+} homeostasis and ER stress [4]. However, no single regimen or combination therapy has been approved by FDA for the treatment of WFS and thus novel therapeutic strategies are urgently needed. Notwithstanding the above, the molecular mechanism underlying β-cell dysfunction in WFS2 has remained elusive. Investigation of mouse models should help by providing mechanistic insights into the pathogenesis of diabetes in WFS2.

[1]Department of Life Sciences and Institute of Genome Sciences, National Yang Ming Chiao Tung University, Taipei 112, Taiwan [2]Department of Biomedical Engineering, College of Engineering, National Cheng Kung University, Tainan 701, Taiwan [3]Center of General Education, Chang Gung University, Taoyuan 333, Taiwan [4]Department of Pharmacology, National Cheng Kung University Hospital, College of Medicine, National Cheng Kung University, Tainan 701, Taiwan [5]The National Genomics Center for Clinical and Biotechnological Applications, Cancer and Immunology Research Center, National Yang Ming Chiao Tung University, Taipei 112, Taiwan [6]Institutes of Physiology, College of Medicine, National Yang Ming Chiao Tung University, Taipei 112, Taiwan [7]Center for Healthy Longevity and Aging Sciences, National Yang Ming Chiao Tung University, Taipei 112, Taiwan [8]Institute of Molecular and Genomic Medicine, National Health Research Institutes, Miaoli 350, Taiwan

[9] Zhao-Qing Shen, Wen-Tai Chiu and Cheng-Heng Kao contributed equally to this work.

*Corresponding author. 155 Li-Nong St., Sec. 2, Peitou, Taipei 11221, Taiwan. E-mail: tftsai@nycu.edu.tw (T.-F. Tsai).

Received November 10, 2024 • Revision received March 24, 2025 • Accepted April 1, 2025 • Available online 4 April 2025

https://doi.org/10.1016/j.molmet.2025.102140

Pancreatic β-cells are specifically designed to sense glucose fluctuations and secrete insulin in response to elevated glucose levels. This facilitates glucose uptake by the liver, skeletal muscle, and adipose tissue, thereby maintaining glucose homeostasis. Insulin synthesis and processing occur via the β-cell secretory pathway, which involves the rough endoplasmic reticulum (ER), Golgi complex and secretory vesicles [5]. The ER plays a central role in secretory protein production and modification, Ca^{2+} homeostasis and cell death signaling. Dysfunction of the ER can trigger a variety of diseases, including diabetes. One important cause of ER stress is ER Ca^{2+} depletion, which results in Ca^{2+} binding chaperone dysfunction, misfolded protein accumulation, and activation of the unfolded protein response (UPR). These ER defects then cause further disturbance of intracellular Ca^{2+} homeostasis. Consequently, in β-cells, ER stress impairs both insulin biosynthesis (via UPR-mediated translational inhibition and proinsulin misfolding) and insulin granule release (via altered Ca^{2+} homeostasis) [6]. The above studies suggest that aberrant Ca^{2+} homeostasis and increased ER stress contribute to β-cell dysfunction thereby potentially leading to atypical diabetes.

Our previous studies have demonstrated that Cisd2 mediates healthy lifespan in mice. Cisd2 deficiency shortens lifespan, causes premature aging and impairs glucose tolerance in Cisd2 knockout (Cisd2KO) mice [7]. CISD2, an integral membrane protein with a CDGSH domain oriented towards the cytosol, is localized to the mitochondrial outer membrane, the ER, and mitochondria-associated ER membranes (MAMs) in a range of cell types [8,9]. The ER and mitochondria are major intracellular Ca^{2+} stores that are able to respond to signals for Ca^{2+} mobilization; furthermore, MAMs serve as hotspots for Ca^{2+} transfer between the ER and mitochondria. Cisd2 plays a crucial role in mitochondrial function and integrity, as well as redox status and intracellular Ca^{2+} homeostasis [9–11]. Importantly, Cisd2 interacts with sarcoendoplasmic reticulum Ca^{2+} ATPase 2 (Serca2), a Ca^{2+} pump that transports Ca^{2+} from cytosol into ER lumen in order to maintain a high ER Ca^{2+} level; this regulates enzymatic activity via modulation of the redox status of Serca2, which, in turn, maintains the level of intracellular Ca^{2+} homeostasis [12,13]. Previous studies have showed that Serca2 deficiency impairs pancreatic β-cell function, disrupting proinsulin processing and maturation, and decreasing glucose-stimulated insulin secretion (GSIS) [14,15]. These studies suggest that Cisd2 is a fundamentally important mediator of cellular homeostasis. However, the role of Cisd2 in β-cell function remains unclear at present.

In this study, our aim was to delineate the essential role of Cisd2 in β-cells and elucidate the molecular mechanism underlying β-cell dysfunction and diabetes, which is a major manifestation of WFS2 and is caused by recessive mutations of CISD2 in patients. To do this, we use β-cell specific Cisd2KO mice, a CRISPR-mediated Cisd2KO MIN6 β-cell line and transcriptomic analysis.

2. RESULTS

2.1. Cisd2 deficiency in β-cells disrupts systemic glucose homeostasis via the impairment of insulin secretion

To study the effects of Cisd2 deficiency on β-cell function, we generated β-cell specific Cisd2KO (Cisd2 βKO) mice by crossing the Ins1-Cre transgenic mice with the Cisd2 floxed (f) mice (Supplementary Figure S1A). The specificity of the Ins1-Cre was validated by crossing the Ins1-Cre mice with CAG-tdTomato reporter mice (Supplementary Figure S1B). Our result confirmed that the Ins1-Cre is specifically expressed in β-cells within the β-islets (Supplementary Figure S1C). Notably, only about 38% of the Cisd2 mRNA levels remained in the β-islets of Cisd2 βKO mice (Supplementary Figure S1D); this agrees approximately with the percentage of non-β-cells (α-cell, δ-cells, PP cells and epsilon-cells) [16]. To study whether Cisd2 deficiency in β-cells causes glucose dyshomeostasis, we performed glucose tolerance tests (GTTs) and insulin tolerance tests (ITTs) (Figure 1A). Interestingly, the basal blood glucose levels are not affected by the KO (Figure 1B); however, an overt phenotype of glucose intolerance was observed in the Cisd2 βKO mice at a young age (3-month old) and during middle age (12-month old) (Figure 1C–E). Importantly, insulin sensitivity remains unchanged (Figure 1F–H), which suggest that glucose dysregulation in these mice may be caused by autonomous cellular dysfunction of β-cells in the Cisd2 βKO mice. Next, we conducted GSIS assays to evaluate β-cell function (Figure 1I). The GSIS of β-cells can be categorized into two phases: the first phase of insulin secretion is generated by fusion of β-granules in the readily releasable pool (RRP) with the cell membrane (within 1–2 min); and the second phase involves translocation of β-granules from the reserve pool (RP) to the RRP to provide expansion and/or replenishment of the RRP (>10 min) [17]. Intriguingly, our results reveal that there are defects during both phases of GSIS in the Cisd2 βKO mice (Figure 1J), indicating that the abnormal glucose intolerance of Cisd2 βKO mice is mainly attributable to the dysfunction of β-cell insulin secretion.

A previous study has revealed that during glucose intolerance, β-cells undergo morphological adaptation to enhance the level of insulin in the plasma; this is an attempt to compensate for the low levels of insulin and thus to maintain glucose homeostasis [18]. To evaluate whether Cisd2 deficiency results in morphological changes to β-islets, we performed histopathological analysis. Remarkably, Cisd2 deficiency in β-cells was found to cause overt hyperplasia and hypertrophy in a portion of the β-islets present (Figure 1K). Quantification of islet size revealed that the number of large size islets (>12,000 μm^2) is significantly increased in the Cisd2 βKO mice compared with Cisd2 f/f mice (Figure 1L). Additionally, a loss of β-cell identity has been reported to be one of the main features of β-cell senescence and age-related diabetes [18]. Interestingly, our immunofluorescence staining revealed that, in the Cisd2 βKO mice, many of the β-cells are glucagon-positive, suggesting that those β-cells have lost their identity and/or have trans-differentiated into α-cell-like cells (Figure 1M). In summary, Cisd2 deficiency in β-cells disrupts glucose homeostasis via an impairment of insulin secretion, which leads to hypertrophy of a proportion of β-islets as a compensatory effect. This results in a loss of identity by some β-cells. Together, these defects appear to bring about glucose intolerance thereby promoting a diabetic-related phenotype.

2.2. Cisd2 βKO causes ultrastructural abnormalities in the ER and mitochondria that disturbs the maturation and secretion of β-granules

To characterize the ultrastructural alterations that may occur in the β-cells of Cisd2 βKO mice, we performed transmission electron microscopy (TEM) analysis before and after treating the mice with glucose (Figure 2A). The insulin secretion pathway involves a number of highly regulated processes, namely insulin biosynthesis, β-granule formation, β-granule maturation and β-granule secretion; all of which can be observed by TEM [16,19] (Figure 2B). In the β-cells of Cisd2 βKO mice at a young age (3-month old), prior to the onset of overt glucose intolerance, TEM revealed that, before glucose treatment, obvious ultrastructural abnormalities, namely mitochondrial degeneration and rough ER dilation, were already detectable (Figure 2C). Notably, after glucose treatment for 15 min, the numbers of mature β-granules and empty vesicles are significantly decreased in the β-cells of Cisd2 βKO mice compared with Cisd2 f/f mice (Figure 2D–E). Furthermore, we quantified the number of mature β-granules located in the different

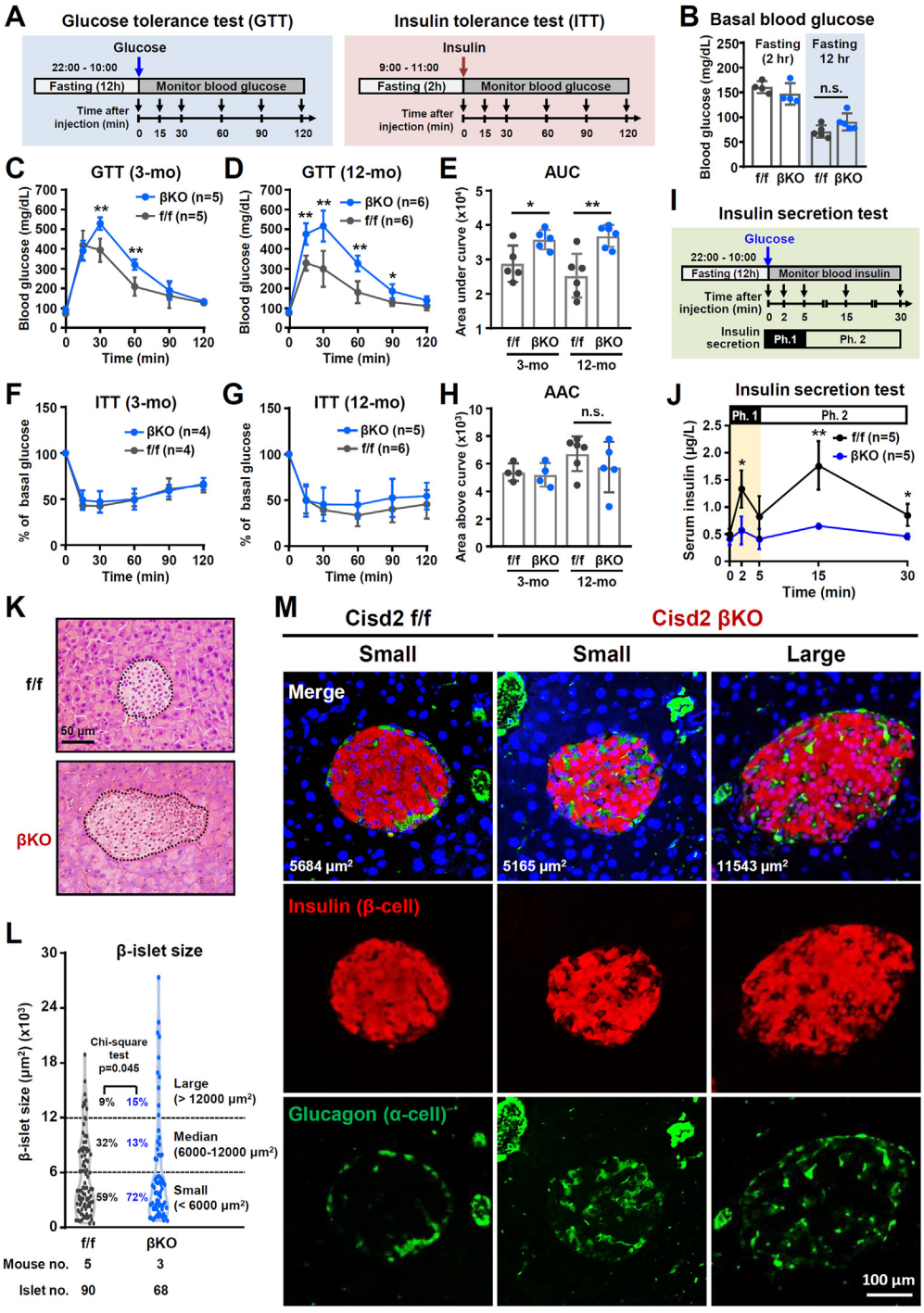

Figure 1: Cisd2 deficiency in β-cells disturbs systemic glucose homeostasis via an impairment of insulin secretion in mice. (A) Protocol used for the oral glucose tolerance tests (GTT) and insulin tolerance tests (ITT). For the oral GTT, mice were orally administrated with glucose water solution (1.5 mg/g body weight) by a feeding needle after 12 h fasting (10 pm−10 am). For the ITT, mice were intraperitoneally injected with insulin (0.75 U/kg body weight) after 2 h fasting (9 am−11 am). Blood samples were collected from tail vein before (0 min) and after the treatment at the indicated time points. **(B)** Basal blood glucose (fasting 2 h and 12 h) levels in the Cisd2 f/f and Cisd2βKO mice at 3-mo old (n = 4−5). **(C−E)** The oral GTT assay for mice at 3-months (C) and 12-months (D) old. The quantification of GTT was carried out by calculating the area under curve (AUC) (n = 5−6) (E). **(F−H)** The ITT assay for mice at 3-months (F) and 12-months (G) old. The quantification of ITT was measured by calculating the area above curve (AAC) (n = 4−6) (H). **(I)** For the insulin secretion test, mice were orally administrated with glucose water solution (1.5 mg/g body weight) by a feeding needle after 12 h fasting (10 pm−10 am). The mouse blood samples were collected before (0 min) and after glucose administrated (2, 5, 15, and 30 min). Phase 1, Ph. 1; Phase 2, Ph. 2. **(J)** Serum insulin levels of Cisd2 βKO and Cisd2 f/f mice at 3-months old. **(K)** H&E staining of the pancreas from male mice at 6-months old. β-islet hypertrophy was found to be present in the pancreas of Cisd2 βKO mice. **(L)** Quantification of β-islet size from histological images. The β-islet size is classified into three subtypes, namely large (>12,000 μm^2), medium (6000−12000 μm^2) and small (<6000 μm^2) and the distribution was then assessed. $*p < 0.05$ by chi-square test. **(M)** Immunofluorescence staining for insulin (red) and glucagon (green) present in pancreas from Cisd2f/f and Cisd2 βKO male mice at 6-months old. Data are presented as mean ± SD. $*p < 0.05$, $**p < 0.005$. The statistical analysis was performed using the Student's t test; not significant (n.s.). (For interpretation of the references to color in this figure legend, the reader is referred to the Web version of this article).

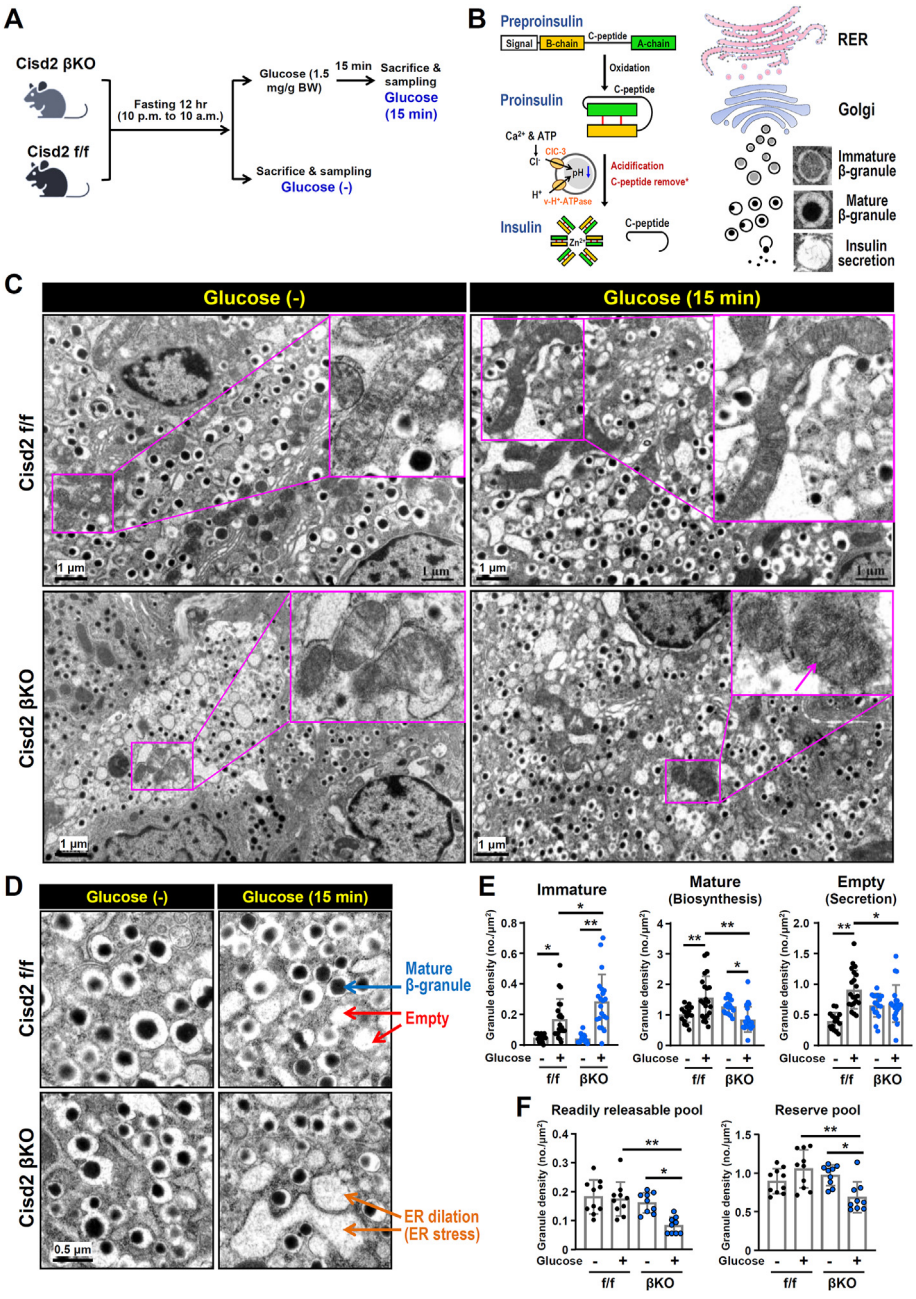

Figure 2: Cisd2 deficiency causes ER dilation and mitochondrial degeneration, as well as disturbing the maturation and secretion of β-granules. (A) Sampling schedule of the ultrastructural analysis of mouse β-islet by TEM. To analyze the glucose-induced insulin secretion, mice were orally administrated with glucose water solution (1.5 mg/g body weight) by a feeding needle after 12 h fasting (10 pm−10 am) and sacrificed before (−) or after 15 min of glucose treatment. **(B)** Schematic diagram of insulin biosynthesis, β-granule maturation and secretion. **(C–D)** Cisd2 deficiency results in ultrastructural abnormalities including rough ER (RER) dilation and mitochondrial degeneration. **(E)** Quantification of β-granule density from the TEM images. Numbers of immature, mature and empty β-granule vesicles were quantified. **(F)** The number of mature β-granule vesicles within the readily releasable and reserve pools were quantified using TEM images. Data are presented as a mean ± SD. $*p < 0.05$, $**p < 0.005$. The statistical analysis was performed using one-way ANOVA with Bonferroni multiple comparison test; not significant (n.s.).

zones of β-cells, namely RRP and RP. Interestingly, after glucose treatment, the numbers of both RRP and RP are significantly reduced in the β-cells of the Cisd2 βKO mice (Figure 2F and Supplementary Figure S2). This result is consistent with the observation that both phase I and phase II of insulin secretion are defective in the Cisd2 βKO mice (Figure 1J). Moreover, quantification of the TEM images revealed a significant increase in ER dilation, a morphological marker of ER stress, in the β-cells of Cisd2 βKO mice compared to Cisd2 f/f mice (Supplementary Figure S3). These results indicate that the impaired GSIS observed in the Cisd2 βKO mice is possibly caused by defects that disturb β-granule maturation and insulin secretion.

2.3. Cisd2 βKO impairs GSIS by causing mitochondrial dysfunction and dysregulation of Ca^{2+}-mediated insulin secretion and this involves multiple processes

Previous studies have revealed that CISD2 maintains cellular function by regulating Ca^{2+} homeostasis [4,9,11,20]. To delineate whether the insulin secretion defect observed in the Cisd2 βKO mice is associated

with Ca^{2+} dysregulation, we examined the ability to secrete insulin when mice are treated with either arginine or gliclazide. These two treatments are able to induce membrane depolarization independent of ATP, which subsequently leads to an extracellular Ca^{2+} influx via the voltage-gated Ca^{2+} channels (VGCCs), thereby enhancing insulin secretion (Figure 3A). Strikingly, a significant reduction in both arginine-stimulated and gliclazide-induced insulin secretion was detected in Cisd2 βKO mice (Figure 3B—D), suggesting that the impaired extracellular Ca^{2+} influx via VGCC is one of the major factors contributing to the insulin secretion defect in Cisd2 βKO mice.

To elucidate the mechanism by which Cisd2 deficiency causes β-cell dysfunction, we used the MIN6 cell line, which is an insulin-secreting β-cell line that retains normal GSIS regulation [21]. Subcellular fractionation of MIN6 β-cells indicates that Cisd2 protein is mainly localized in the ER and mitochondria (Supplementary Figures S4A—B). A MIN6-Cisd2KO cell line was generated using the CRISPR/Cas9-mediated method to delete a genomic region covering the start codon of the Cisd2 gene (Supplementary Figure S4C). Complete absence of the Cisd2 protein was confirmed by Western blot analysis of the MIN6-Cisd2KO cells (Supplementary Figure S4D). The regulation

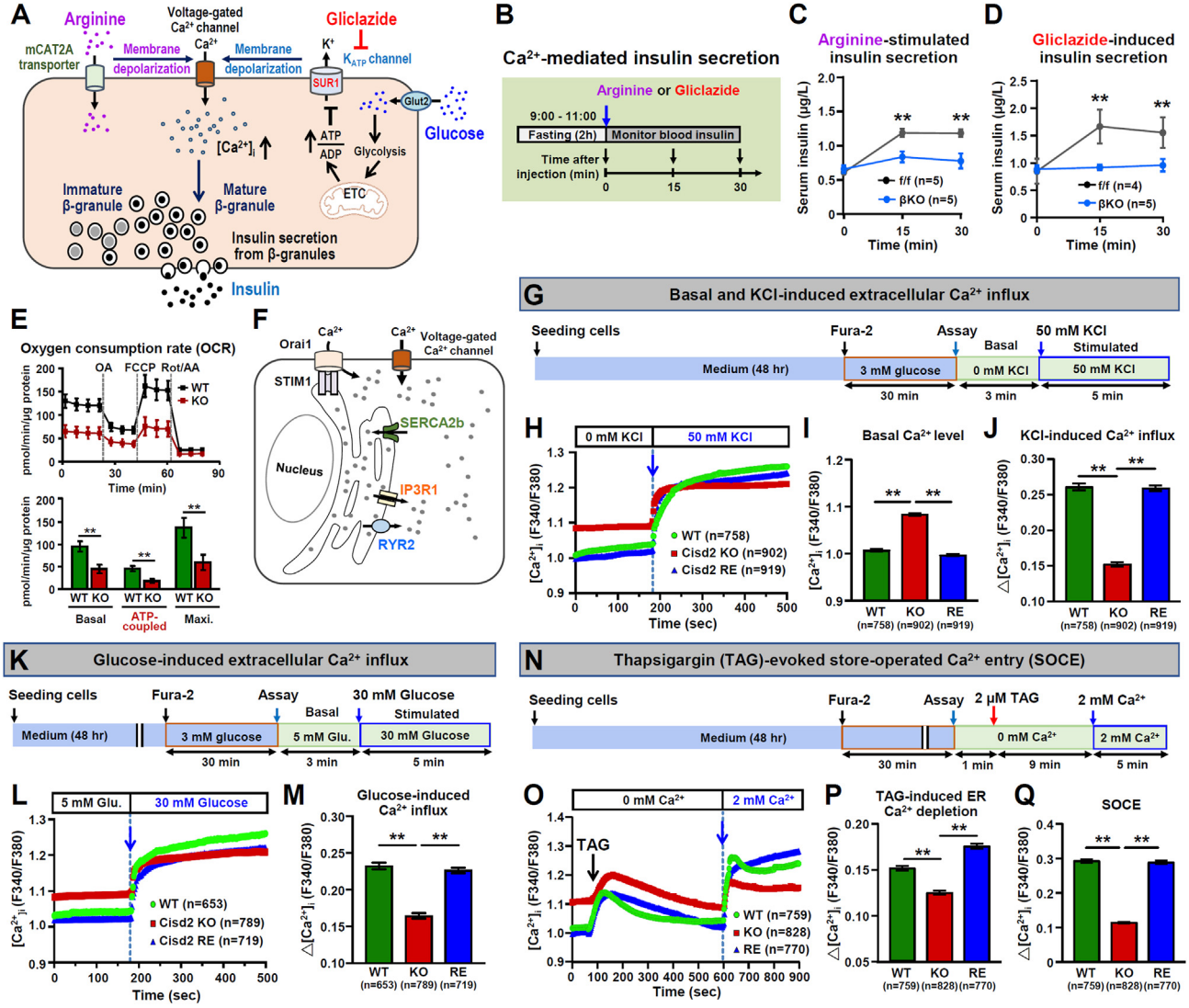

Figure 3: Cisd2 deficiency in mice (the MIN6 β-cell line) disrupts Ca^{2+}-mediated insulin secretion, impairs mitochondrial function and disturbs intracellular Ca^{2+} homeostasis. (A) Schematic diagram of Ca^{2+}-mediated insulin secretion in β-cell. Arginine treatment can stimulate membrane depolarization of β-cells. Gliclazide is a second-generation sulfonylurea that can inhibit K_{ATP} channels leading to membrane depolarization in β-cells. **(B)** For the Ca^{2+}-mediated insulin secretion test, mice were intraperitoneally injected with arginine (0.3 g/kg body weight) or gliclazide (10 mg/kg body weight) after 2 h fasting (9 am—11 am). The mouse blood samples were collected before (0 min) and after arginine or gliclazide administrated (15 and 30 min). **(C)** Significant decreases in arginine-stimulated insulin secretion by the Cisd2 βKO mice at 3-months old. **(D)** Significant decreases in gliclazide-induced insulin secretion by the Cisd2 βKO mice at 3-months old. $*p < 0.05$, $**p < 0.005$. The statistical analysis was performed using Student's t test. **(E)** Decreased mitochondrial oxygen consumption rate (OCR) in MIN6-Cisd2KO cells. **(F)** Schematic diagram of intracellular Ca^{2+} regulation in β-cells. **(G)** Protocol for KCl-induced extracellular Ca^{2+} influx. **(H—J)** Significant increases in the basal cytosolic Ca^{2+} levels. Significant decreases in KCl-induced extracellular Ca^{2+} influx in the MIN6-Cisd2KO cells. **(K)** Protocol for assessing glucose-induced extracellular Ca^{2+} influx. **(L—M)** Significant decreases in glucose-induced extracellular Ca^{2+} influx in MIN6-Cisd2KO cells. **(N)** Protocol for thapsigargin (TAG)-evoked store-operated calcium entry (SOCE). **(O—Q)** Significant decreases in TAG-induced Ca^{2+} depletion and TAG-evoked SOCE in MIN6-Cisd2KO cells. Levels of cytosolic Ca^{2+} in single MIN6 β-cells were measured by fluorescence microscopy using Fura-2/AM staining. $*p < 0.05$, $**p < 0.005$. In C-E, data are presented as mean ± SD. In H—J, L, M, O—Q, data are presented as mean ± SEM.

of GSIS involves multiple processes, namely glucose uptake, glycolysis, mitochondrial ATP production, membrane depolarization and Ca^{2+} signaling [16]. Intriguingly, in the MIN6-Cisd2KO cells, a significant decrease in the cells' mitochondrial oxygen consumption rate (OCR), including basal OCR, ATP-coupled OCR, and maximal OCR, was detected, which suggests that Cisd2 deficiency impairs mitochondrial ATP production (Figure 3E).

Intracellular Ca^{2+} homeostasis is regulated by several Ca^{2+} channels present in the ER (SERCA2b, IP3R1, RYR2 and STIM1) and in the plasma membrane (Orai1 and VGCC) (Figure 3F). Previous studies have demonstrated that dysregulation of SERCA2b and VGCC results in β-cell dysfunction and insulin secretion defects [6]. Experimentally, the addition of KCl leads to an increase in extracellular [K^+], which causes membrane depolarization, and then opens the VGCC channel (Figure 3A); and this in turn increases cytosolic [Ca^{2+}]. Notably, in the MIN6-Cisd2KO cells, a significant elevation of basal cytosolic [Ca^{2+}] was detected. Additionally, Cisd2 deficiency impaired the KCl-induced extracellular Ca^{2+} influx, which results in a significant reduction of the KCl-induced [Ca^{2+}] influx (Figure 3G—J). Consistent with the above, similar phenomena were observed when glucose-induced extracellular Ca^{2+} influx was measured (Figure 3K—M). Moreover, in the MIN6-Cisd2KO cells, both the thapsigargin (TAG)-evoked ER-releasable Ca^{2+} and store-operated calcium entry (SOCE) were found to be significantly impaired (Figure 3N—Q).

To confirm that the phenotypic defects of the MIN6-Cisd2KO cells are indeed caused by Cisd2 deficiency rather than an off-target effect, we generated MIN6-Cisd2RE cells in which Cisd2 is re-expressed in MIN6-Cisd2KO cells using the lentivirus-mediated method (Supplementary Figure S4E). In addition, Western blot analyses revealed that an ER stress marker, namely the phosphorylated form of eIF2α (p-eIF2α), is significantly elevated in the MIN6-Cisd2KO cells; and that this can be rescued by Cisd2 re-expression in the MIN6-Cisd2RE cells (Supplementary Figures S4F—G). Importantly, in the MIN6-Cisd2RE cells, the defects associated with Ca^{2+} dysregulation, namely the basal cytosolic Ca^{2+} level, glucose-induced and KCl-induced extracellular Ca^{2+} influx (Figure 3G—M), together with the TAG-evoked SOCE (Figure 3N—Q), all disappeared. Obviously, the MIN6-Cisd2RE cells have reverted to a situation similar to that in the MIN6-WT cells. Thus, this re-repression study demonstrated that the Ca^{2+} dysregulation present in the MIN6-Cisd2KO cells is indeed caused by Cisd2 deficiency. In summary, these studies reveal that Cisd2 deficiency leads to an impairment of extracellular Ca^{2+} influx, which then compromises Ca^{2+}-mediated signaling, and causes mitochondrial dysfunction; the end point being impaired insulin secretion by β-cells.

To investigate if manipulating the ER stress-related signaling pathway is able to influence the phenotypes associated with intracellular Ca^{2+} dysregulation, and to determine if inhibition of ER stress can rescue the Ca^{2+} dysregulation caused by Cisd2 deficiency, we performed Ca^{2+} measurement and image analysis on the MIN6-WT, MIN6-Cisd2KO and MIN6-Cisd2RE cells. These cells were treated with either the PERK inhibitor GSK2606414 (an ER stress inhibitor) or the eIF2α dephosphorylation inhibitor Salubrinal (an ER stress inducer) (Supplementary Figure S5). In the MIN6-WT cells, Salubrinal-induced ER stress causes dysregulation of Ca^{2+} homeostasis, characterized by elevated basal cytosolic Ca^{2+} levels, a significant decrease in TAG-induced ER Ca^{2+} depletion and impairment of TAG-evoked SOCE. These results suggest that ER stress directly disrupts intracellular Ca^{2+} homeostasis in the MIN6-WT cells. Intriguingly, in the MIN6-Cisd2KO cells, inhibition of ER stress by GSK2606414 is able to rescue the Ca^{2+} dysregulation. Furthermore, in the MIN6-Cisd2RE cells, all Ca^{2+}-related phenotypes are comparable to those in the MIN6-WT cells (Supplementary Figure S5). Together, these results reveal that the Ca^{2+} dysregulation in the MIN6-Cisd2KO cells is likely occur via the ER stress-related PERK-eIF2α signaling pathway.

2.4. Transcriptomics revealed that Cisd2 modulates proteostasis and the ER, mitochondrial function, insulin secretion and vesicle transport, all of which are involved in maintaining β-cell function

To explore the molecular mechanisms underlying the role of Cisd2 in β-cell function, we perform RNA sequencing (RNA-seq) and pathway analysis on the β-islets from Cisd2 f/f and Cisd2 βKO mice under glucose-stimulated insulin secretion conditions (Figure 4A). The mRNA expression levels of 8,616 genes were quantified. Principal component analysis (PCA) indicates a dramatic difference in transcriptomic profiles between the β-islets of Cisd2 f/f and the β-islets of Cisd2 βKO mice (Figure 4B). A pair-wise differentially expressed gene (DEG) analysis was performed. Normalized counts and DEGs were obtained using DESeq2 (using the Wald test) with a false discovery rate (FDR) < 0.05 (Cisd2 βKO *vs.* Cisd2 f/f). This analysis identified a total of 1,026 DEGs (up-regulated 550 DEGs; down-regulated 476 DEGs) (Figure 4C).

The DEGs were further annotated by enrichment analysis using Gene Ontology (GO) and KEGG. Interestingly, the DEGs are mainly involved in pathways related to β-cell survival and function, namely proteostasis and ER stress, metabolism, mitochondrial function and stress response, insulin secretion and vesicle transport, Ca^{2+} signaling, cell death, and a number of signaling pathways (Figure 4D—E and Supplementary Figure S6). Specifically, in terms of insulin secretion and vesicle transport, the following processes were identified: response to glucose ER to Golgi-mediated vesicle transport; Ca^{2+}-mediated signaling; and regulation of insulin secretion (Supplementary Figure S6C). Additionally, pathways associated with insulin-dependent diabetes (maturity onset diabetes of the young) and senescence are enriched in the β-islets of Cisd2 βKO mice (Supplementary Figure S6D). Notably, down-regulation of several glucose sensing machinery-related enzymes (Glut2, Gck and Pkm), and various tricarboxylic acid (TCA) cycle-related enzymes (Pcx and Idh2), Ca^{2+} pumps (Serca2 and Serca3) and Ca^{2+} channels (VGCCs), as well as upstream regulators of Ca^{2+} signaling pathways, were also found among the DEGs of the Cisd2KO β-islets (Supplementary Figure S7). Consistently, KEGG indicates that the identified DEGs are involved in a number of pathways associated with diabetes and aging (Figure 4E). Moreover, Ingenuity Pathway Analysis (IPA; $p < 0.05$ & absolute Z score > 0.5) of the DEGs identified four major functional groups. These are: (1) β-cell function and development; (2) β-cell homeostasis-related signaling pathways; (3) proteostasis and ER stress; and (4) mitochondrial function and autophagy (Figure 4F). Intriguingly, pathways associated with pancreatic β-cell dysfunction, inflammation and stress response, including non-canonical NF-κB signaling, UFMylation and the KEAP1-NRF2 pathways [22—25], are also significantly activated in the β-islet of Cisd2 βKO mice (Figure 4F). Conversely, pathways related to β-cell function, maintenance and stress protection, including DHCR24, AMPK, PDGF, EGF and HIF1α [26—30], are significantly suppressed in the β-islets of Cisd2 βKO mice.

These transcriptomic results suggest that Cisd2 maintains β-cell function and homeostasis via the regulation of proteostasis, mitochondrial function, insulin secretion and vesicle transport. Moreover, these findings are also consistent with the phenotypic observations obtained regarding Cisd2 βKO mice and MIN6-Cisd2KO cells in terms of glucose intolerance, defective insulin secretion (Figure 1C—E, 1J and Figure 3A—D), ER stress (Figure 2D and Supplementary Figure S3 and S4F-G), mitochondrial dysfunction (Figure 3E), and disrupted intracellular Ca^{2+} homeostasis (Figure 3F—Q).

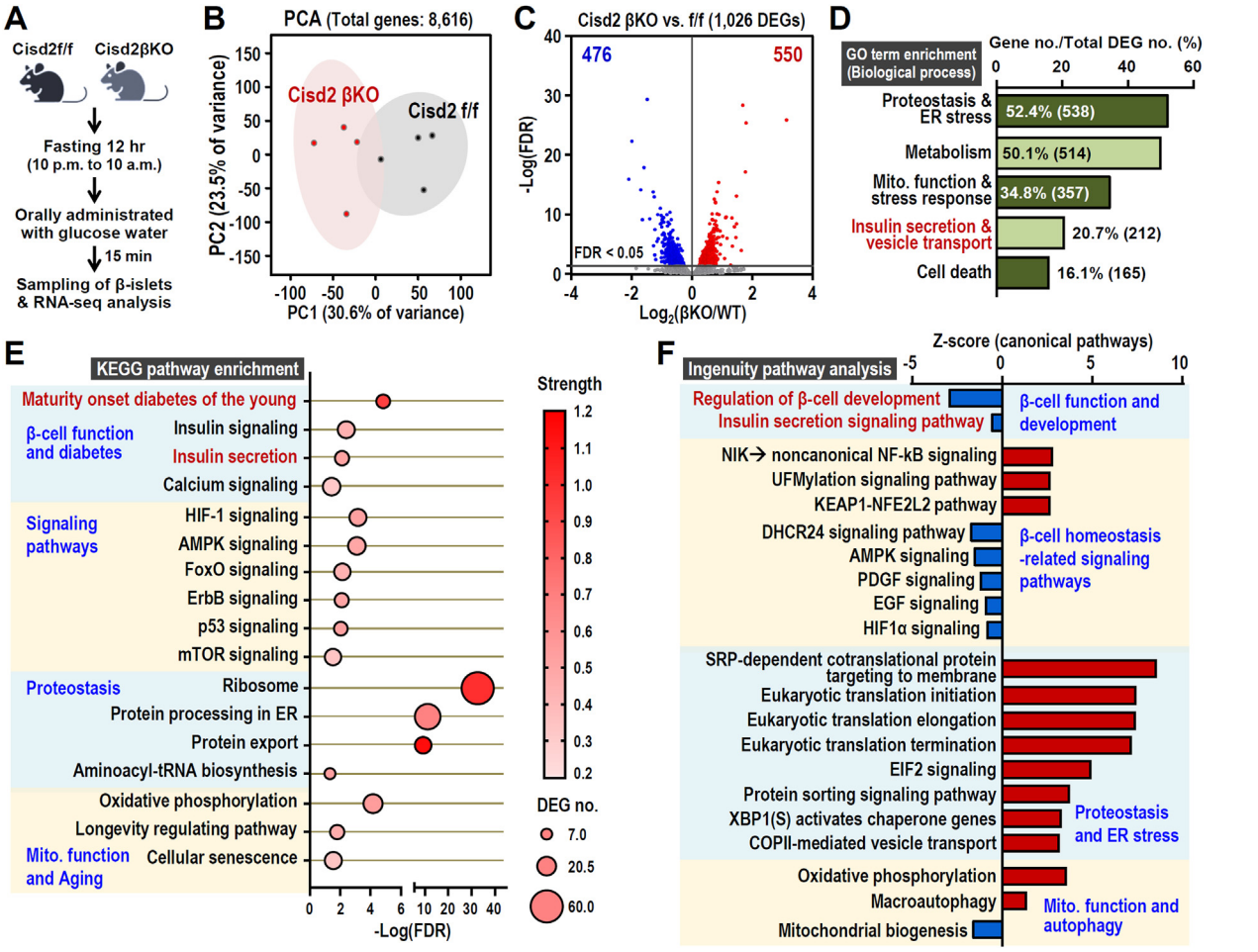

Figure 4: Transcriptomic analysis of the β-islets reveals that Cisd2 modulates proteostasis and ER, mitochondrial function, insulin secretion and vesicle transport in order to maintain β-cell functioning. (A) Cisd2 f/f and Cisd2 βKO mice at 3-months old were orally administrated with glucose water solution (1.5 mg/g body weight) by a feeding needle after 12 h fasting (10 pm—10 am) and sacrificed after 15 min of glucose administration. Total RNAs were isolated from the β-islets of the mice. **(B)** Principal component analysis (PCA) of all transcriptomic data (total expressed 8,616 genes) in the β-islets of Cisd2 f/f and Cisd2 βKO mice (n = 4). **(C)** Volcano plot revealing transcriptome changes (Cisd2 βKO *vs.* f/f). Horizontal line shows the 5% false discovery rate (FDR) threshold. Red or blue plots identify genes above the indicated FDR threshold. A total of 1,026 DEGs are affected by Cisd2 deficiency (550 up-regulated and 476 down-regulated genes; Cisd2 βKO *vs.* f/f, FDR < 0.05). **(D)** The biological processes obtained from the Gene Ontology (GO) annotation of the transcriptome changes (1,026 DEGs) between β-islets of Cisd2βKO and f/f mice. The DEGs are grouped into proteostasis and ER stress, mitochondrial (Mito.) function and stress response, insulin secretion and vesicle transport and cell death associated pathways; the results are presented as a percentage of the total DEG number. **(E)** A bubble plot illustrating the enrichment analysis of KEGG pathway DEGs between the β-islets of Cisd2βKO and f/f mice. The grouping of the GO annotation and KEGG pathways were carried out by STRING v11.5 (https://string-db.org/). Pathway FDR < 0.05. **(F)** Canonical pathway analysis by Ingenuity Pathway Analysis (IPA) software using the transcriptome changes in the β-islets of Cisd2βKO mice (Cisd2βKO *vs.* f/f; pathway *p*-value < 0.05 and absolute Z-score > 0.5). (For interpretation of the references to color in this figure legend, the reader is referred to the Web version of this article).

2.5. The activation state of two potential upstream regulators, Glis3 and Hnf1a, was found to be suppressed under Cisd2 deficiency

To explore the potential upstream regulators of the DEGs, we performed upstream analysis using IPA. We identified two up-regulated and six down-regulated upstream regulators ($p < 0.05$ and absolute Z score > 2; Supplementary Table S1). Intriguingly, the predicted activation state of two these transcription factors that are involved in β-cell function, namely Glis3 and Hnf1a [31—34], was significantly inhibited in the β-islets of Cisd2 βKO mice. Glis3 is known to activate various genes involved in insulin biosynthesis and secretion, as well as β-cell function and identity. Most of the downstream target genes of Glis3 were down-regulated in the β-islets of Cisd2 βKO mice (Figure 5A—B and Supplementary Figures S8A—D). Specifically, among the target genes of Glis3, several regulators of β-cell function and identity (Mafa, Neurod1, Pdx1, NKX6.1 and Isl1) [18,35] are significantly decreased; in addition, the genes responsible for insulin biosynthesis and secretion (Ins1, Ins2 and Glut2) are also significantly decreased (Figure 5B). Similarly, Hnf1a regulates a variety of target genes that modulate glucose metabolism, pancreas development, membrane depolarization and vesicle transport and most of these target genes are also down-regulated in the β-islets of Cisd2 βKO mice (Figure 5C—D and Supplementary Figures S8E—J). It is worth mentioning that Glut2 (glucose transporter 2) is a downstream target gene of both Glis3 and Hnf1a. Glut2 is a glucose sensor present in pancreatic β-cells and is an essential protein for the functioning of the GSIS [36]. Expression of this gene is significantly decreased when there is Cisd2 deficiency (Figure 5A,C and Supplementary Figure S8C). Importantly, in humans, loss-of-function mutations in GLIS3, HNF1a, NEUROD1, PDX1 and INS have been reported to be associated with the pathogenesis of monogenic diabetes [2,34,37]. To validate these

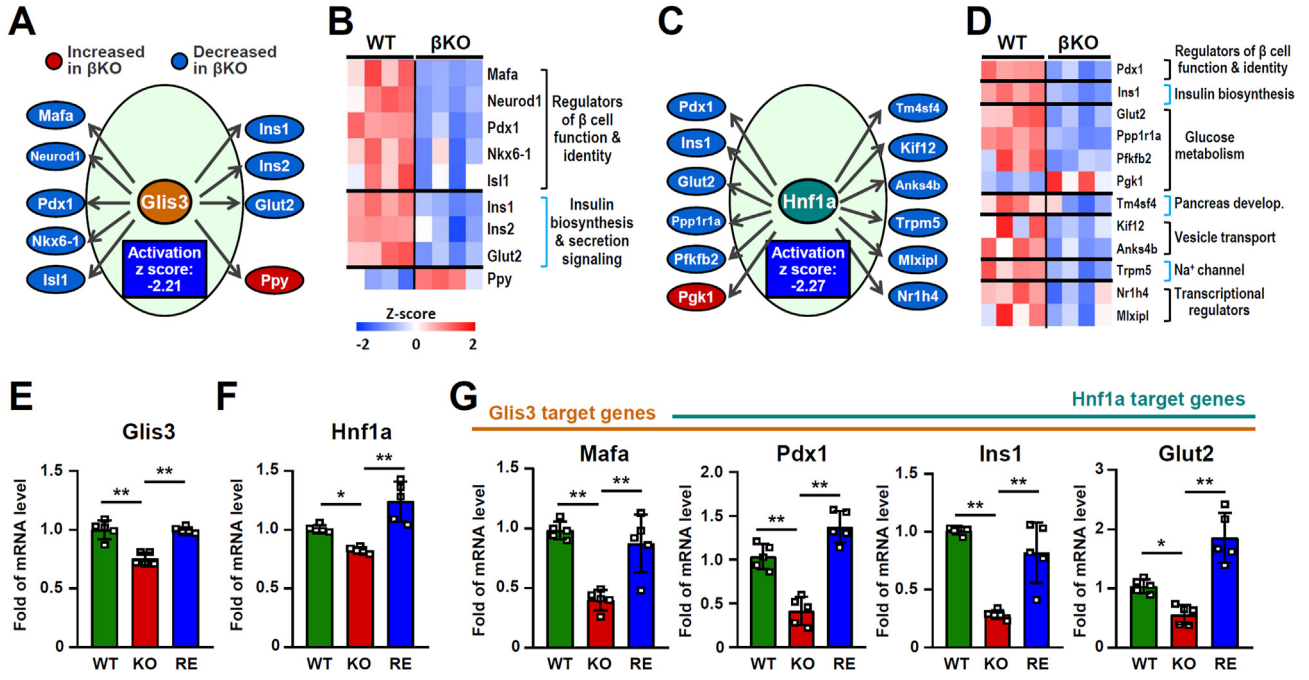

Figure 5: Activation state of two potential upstream regulators, Glis3 and Hnf1a, was suppressed under Cisd2 deficiency. (A—B) Significant inhibition of Glis3 transcriptional signaling based on the activation z-scores (z-score < -2.0 and p-value < 0.05) and the IPA upstream regulator analysis of the DEGs identified in the β-islets of Cisd2 βKO mice. Most of the mRNA levels of Glis3 downstream target genes are significantly downregulated under Cisd2 deficiency. The DEGs can be classified according to their functions as regulators of β cell function and identity and as regulators of insulin biosynthesis and insulin secretion signaling. **(C—D)** Significant inhibition of Hnf1a transcriptional signaling based on activation z-score (z-score < -2.0 and p-value < 0.05) and the IPA upstream regulator analysis of the DEGs in the β-islets of Cisd2 βKO mice. Most of the mRNA levels of Hnf1a downstream target genes are significantly down-regulated under Cisd2 deficiency. The DEGs can be classified according to their functions as being involved in glucose metabolism DEGs, amino acid transport DRGs and metabolism DEGs, pancreas development (develop.) DEGs, vesicle transport DEGs, Na^+ channel genes involved in insulin secretion, transcriptional regulators and more. **(E)** The mRNA levels of Glis3. **(F)** The mRNA levels of Hnf1a. **(G)** The mRNA levels of Mafa, Pdx1, Ins1 and Glut2. In (E)—(G). There are five independent biological replicates (n = 5) for each genotype of the cells. The mRNA levels were quantified by real-time RT-qPCR. Data are represented as mean ± SD. $*p < 0.05$, $**p < 0.005$. The statistical analysis was performed using one-way ANOVA with the Bonferroni multiple comparison test.

findings, we examine the mRNA levels of Glis3 and Hnf1a, as well as their downstream target genes, by real-time RT-qPCR. Interestingly, in the MIN6-Cisd2KO cells, Cisd2 deficiency results in down-regulation of Glis3, Hnf1a, and theirs downstream target genes, including Mafa, Pdx1, Ins1 and Glut2. Furthermore, in the MIN6-Cisd2RE cells, the expression profiles of these genes are similar to that in the MIN6-WT cells but distinct from that in the MIN6-Cisd2KO cells (Figure 5E—G). A graphic summary of the DEGs and the pathways associated with the insulin secretion defect in the β-cells of Cisd2 βKO mice is provided; this illustrates that the defects occur in a range of processes when Cisd2 deficiency is present (Figure 6).

3. DISCUSSION

Here we provide evidence to demonstrate the essential role of Cisd2 in β-cells and, furthermore, we delineate the molecular mechanism underlying β-cell dysfunction and diabetes in WFS2 individuals using a mouse model. Four findings are pinpointed. Firstly, Cisd2 deficiency in β-cells disrupts systemic glucose homeostasis via an impairment of β-granules synthesis and insulin secretion; this causes hypertrophy of the β-islets and a loss of identity of a proportion of β-cells in the Cisd2 βKO mice. Secondly, Cisd2 deficiency leads to the impairment of glucose-induced extracellular Ca^{2+} influx, which compromises Ca^{2+}-mediated insulin secretory signaling, and causes mitochondrial dysfunction; this, in turn, impairs insulin secretion in MIN6-Cisd2KO cells. Thirdly, transcriptomic analysis of the β-islets reveals that Cisd2 modulates proteostasis and ER stress, regulates mitochondrial function, as well as mediating insulin secretion and vesicle transport, in order to maintain β-cell function. Finally, the activated state of two potential upstream regulators, Glis3 and Hnf1a, was found to be significantly suppressed under Cisd2 deficiency. The downstream target genes of Glis3 and Hnf1a are heavily involved in β-cell function and identity, namely insulin biosynthesis, vesicle transport and secretion, and glucose metabolism, as well as pancreas development. These findings provide mechanistic insights and form an experimental basis for the development of new therapeutic strategies aimed at the effective treatment of diabetes in WFS2 individuals.

3.1. CISD2 modulates Ca^{2+}-dependent insulin secretion in β-cells

Previous studies have revealed that Cisd2 deficiency dysregulates intracellular Ca^{2+} homeostasis across a variety of cell types, including hepatocytes, cardiomyocytes, neurons, human corneal epithelial cells, and WFS2 patient-derived fibroblasts [8,12,13,38—42]. In this context, it seems that Cisd2 interacts with a range of Ca^{2+} handling proteins in the ER, including SERCA, IP3R1, RyR2, Gimap1, and Calnexin, in order to maintain Ca^{2+} homeostasis and ER function [4,9,41,42]. Specifically, we have demonstrated that Cisd2 directly binds to SERCA2 to maintain its redox status. Thus, Cisd2 deficiency results in an increase in the oxidative modification of SERCA2; this in turn leads to a decrease of enzymatic activity of SERCA2 when pumping Ca^{2+} from cytosol into ER. As a result, Ca^{2+} is accumulated in the cytosol, while at the same time the level of ER Ca^{2+} is dramatically reduced. Subsequently, the

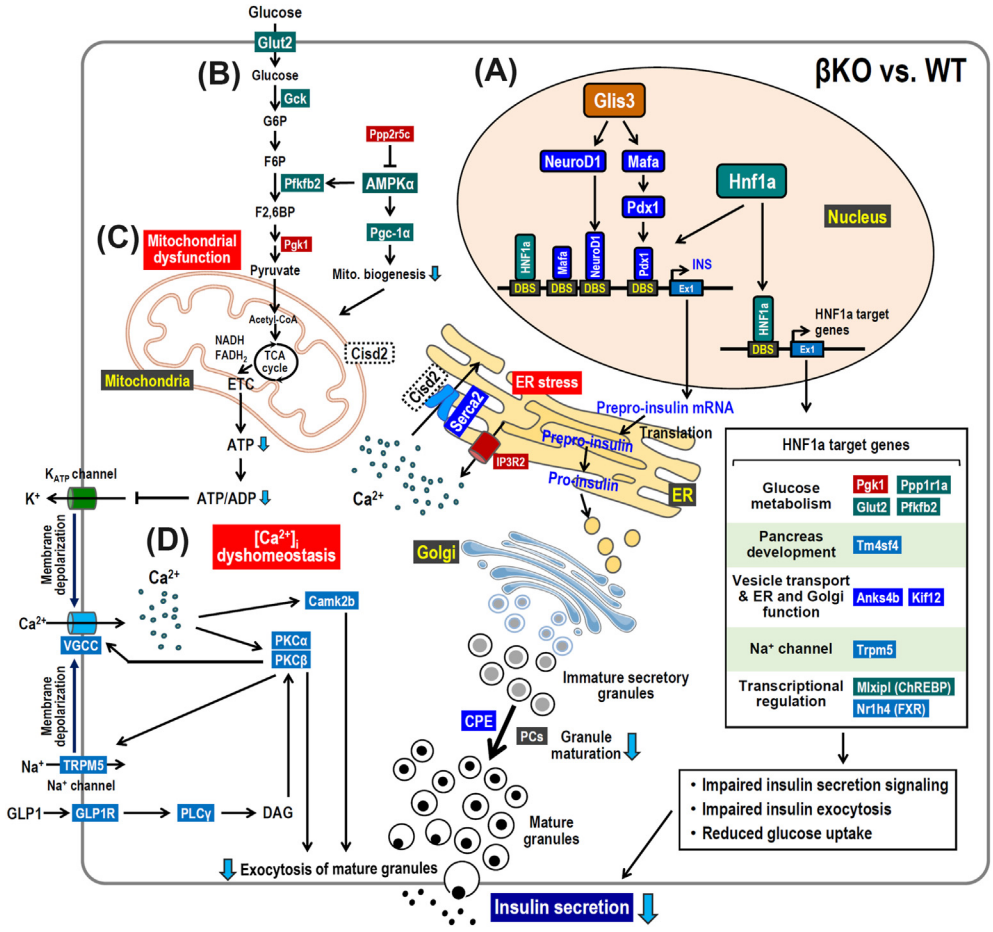

Figure 6: A graphic summary of the DEGs and pathways associated with the insulin secretion defect in the β-cells of Cisd2 βKO mice. (A) Cisd2 deficiency leads to suppression of Glis3 and Hnf1a, which are transcriptional regulators involved in β-cell functioning and identity. This, in turn, leads to downregulation of their target genes thereby impairing glucose uptake and the signaling associated with insulin biosynthesis and secretion. Moreover, Cisd2 deficiency causes ER stress, which then disturbs the maturation process of the β-granules. **(B)** Cisd2 deficiency results in downregulation of glucose transporter Glut2 expression leading to a decrease in glucose uptake and decreased ATP production. In addition, inhibition of AMPKα-Pgc-1α signaling, which is involved in mitochondrial biogenesis, is present in Cisd2KO-MIN6 β-cells and this is likely to contribute to mitochondrial dysfunction. **(C)** Cisd2 deficiency causes mitochondrial dysfunction and reduces ATP production thereby decreasing the ATP/ADP ratio; consequently, this disrupts K_{ATP} channel-mediated membrane depolarization and impairs Ca^{2+} influx in β-cells. **(D)** Downregulation of VGCC and various Ca^{2+}-related signaling pathways, namely PLCγ, Camk2b and PKC, may further contribute to defects in exocytosis of insulin from β-granules. Together, all these defects, which are occurring in multiple processes and in various stages of insulin biogenesis/secretion, result in β-cell dysfunction within the Cisd2 βKO mice. Red boxes indicate upregulation of the mRNA levels; green and blue boxes indicate downregulation of the mRNA levels. (For interpretation of the references to color in this figure legend, the reader is referred to the Web version of this article).

elevated cytosolic Ca^{2+} enters the mitochondria, leading to mitochondrial Ca^{2+} overload thereby damaging mitochondrial function. Additionally, the abnormal elevation of the cytosolic Ca^{2+} level appears to activate various Ca^{2+}-dependent signaling pathways, namely calpain-caspase 3 signaling, calcineurin signaling, and calmodulin-protein kinase C (PKC) signaling [20,38,43]. This then results in adverse effects on cell survival. Intriguingly, targeting the Ca^{2+}-dependent signaling pathways has been shown to alleviate the defects caused by Cisd2 deficiency [20,38]. In this study, we show that, in β-cells, Cisd2 deficiency disrupts Ca^{2+} homeostasis and causes Ca^{2+}-mediated insulin secretion defects. Accordingly, targeting the Ca^{2+}-dependent signaling pathways could be a novel strategy for treating insulin-dependent diabetes in WFS2 individuals.

The secretion of insulin by β-cells is directly regulated by Ca^{2+} via the fusion of β-granules with the cell membrane. Cisd2 deficiency reduces the level of circulating insulin when this is stimulated by glucose (Figure 1J), arginine (Figure 3C) or gliclazide (Figure 3D) in Cisd2 βKO mice. These effects can be explained by the regulation of Ca^{2+} by Cisd2. Normally, in the first phase of insulin secretion, VGCC-mediated extracellular Ca^{2+} influx causes an increase in cytosolic Ca^{2+} and promotes insulin release. The cytosolic Ca^{2+} surge then triggers RyR activation, which releases Ca^{2+} from the ER into the cytosol (Ca^{2+}-induced Ca^{2+} release, CICR). This further activates the SOCE, which promotes the second phase of insulin secretion. In MIN6-Cisd2KO cells, Cisd2 deficiency causes a reduction in the VGCC-mediated extracellular Ca^{2+} influx brought about by KCl (Figure 3G—J) or glucose (Figure 3K—M). Ultimately this leads to a reduction in the first phase of insulin secretion (Figure 1J). In addition, Cisd2 deficiency causes decreased SERCA activity, which will bring about a simultaneous decrease in the scale of TAG-induced ER releasable Ca^{2+} (Figure 3O—P) and SOCE (Figure 3O,Q). Eventually this leads to a reduction in the second phase of insulin secretion (Figure 1J).

Furthermore, ER Ca^{2+} depletion due to the inhibition of SERCA activity seems to cause ER stress and increase the number of immature β-granules (Figure 2E).

3.2. Wfs1 KO and Cisd2 KO mice share common pathogenic process in β-cells

Loss-of-function mutations in the genes WFS1 (wolframin) and CISD2 cause WFS1 and WFS2 in humans, respectively [4]. Previous studies showed that knockout of Wfs1 in mice leads to hyperglycemia via impairing insulin production and secretion from β-cells, thus causing β-cell loss in β-islets. Moreover, β-cell dysfunction and death are caused by disrupted intracellular Ca^{2+} homeostasis, ER stress and calpain hyperactivation [1]. In the INS-1 β-cell line having Wfs1 overexpression, transcriptomic analysis has revealed that WFS1 maintains β-cell function by enhancing the expression of insulin and several β-cell maturity factors, such as Nkx2.2 and Nkx6.1, and by suppressing ER stress-related pro-apoptotic pathways (e.g. Chop-Trib3-Caspase 3 axis) [44]. Interestingly, Wfs1 KO and Cisd2 KO mice have several phenotypes in common, including glucose dyshomeostasis, β-cell dysfunction, elevated cytosolic Ca^{2+} levels, ER stress and abnormal alterations to the transcriptome. These phenotypic overlaps suggest that Cisd2 is likely to have a convergent role that functionally interacts with Wfs1 in β-cells [4]. Notably, a recent study indicated that Cisd2 overexpression can partially rescue the Ca^{2+} dysregulation found in Wfs1-deficient neurons [42]. Thus, it is possible that there are similarities between the pathogenic process involved in β-cell dysfunction and insulin-dependent diabetes in both WFS1 and WFS2.

3.3. Translational perspective of atypical diabetes in WFS

Currently, there is no effective treatment to retard or reverse the progression of WFS. Recent clinical and pre-clinical studies have focused on targeting the following: (a) ER Ca^{2+} stabilizers such as Dantrolene, Ibudilast and Sitagliptin; (b) drugs that reduce ER stress such as Valproate, a GLP-1 receptor agonist; and (c) chemical chaperones such as 4-phenylbutyric acid and tauroursodeoxycholic acid [1,45,46]. However, despite these ongoing trials, no single regimen or combination has been approved by FDA for treating WFS. Thus, new approaches and novel therapeutics are needed.

Intriguingly, a recent study has shown that overexpression of SERCA2b or treatment with CDN1163 (an allosteric SERCA activator) can rescue intracellular Ca^{2+} dysregulation, namely ER Ca^{2+} depletion and cytosolic Ca^{2+} elevation, in both Wfs1 and Cisd2 deficient primary neurons [42]. Notably, down-regulation of Serca2b expression has been observed in β-cells of diabetic patients and db/db mice [47,48]. CDN1163 treatment has been shown to increase insulin synthesis and exocytosis, as well as promoting mitochondrial function in the β-islets obtained from WT mice and MIN6 β-cells. Moreover, In the context of disease, CDN1163 ameliorates palmitate-induced insulin secretory defects, lipotoxicity and trimethylamine N-oxide-induced β-cell dysfunction [47–49]. Additionally, treatment with a GLP-1 receptor agonist has improved glucose homeostasis in a WFS2 patient and it was also found to enhances GSIS in INS-1 β-cells with Cisd2 KD [50]. These results suggest that a pharmacological restoration of Ca^{2+} homeostasis could be an effective therapeutic strategy when treating WFS.

Moreover, several naturally-derived polyphenols have been identified as SERCA activators [51]. Therefore, the evaluation of the therapeutic potentials of these polyphenols will be of great interest. Such an approach for WFS could involve using MIN6-Cisd2KO as a cell platform and Cisd2 βKO mice as a pre-clinical model.

3.4. Limitations and perspectives

Two potential upstream regulators, Glis3 and Hnf1a, have been identified and found to be significantly down-regulated when Cisd2 deficiency is present. These two transcription factors play crucial roles in β-cell function and identity. However, the connection between Cisd2 and the activation of Glis3 and Hnf1a remains unclear. Accordingly, it will be of great importance to study the mechanism underlying the Cisd2-mediated regulation of Glis3 and Hnf1a.

In addition, in the Cisd2 βKO mice, we did not observe glycosuria until they became middle aged at 12-mo old. This may be attributed to the genetic background of these mice, since C57BL/6 is a diabetes-resistant strain [52]. Therefore, further studies evaluating the phenotypes of Cisd2 βKO mice in a diabetes-susceptible strain, such as the DBA/2J, will be of great interest. Furthermore, Cisd2 βKO mice are able to serve as an animal model to examine the synergistic effects of Cisd2 deficiency and Western diet-induced glucose dysregulation. This may help to pinpoint the interplay between atypical diabetes and the metabolic dysfunction induced by a high-fat and high-sugar diet.

Regarding the human relevance of this study, currently this area remains unexplored and warrants further investigation. Although the phenotypes related to β-cell function are similar between WFS patients and mouse models, specific research focusing on WFS2 remains limited. In addition, mechanistic studies underlying the pathogenesis of WFS have predominantly utilized WFS1-related mouse and cell models [53]. Previously iPSC-derived β-cells from patients with diabetes has been demonstrated to have a potential to be used in a mechanistic study; such an approach would involve gene editing and cell therapy evaluation [54]. It will be of great interest in the future to carry out a mechanistic study involving human CISD2 and then move on to an evaluation of novel therapeutic agents that might have been identified through translational research using an iPSC-induced β-cell model derived from WFS2 patients.

4. MATERIALS AND METHODS

4.1. Mouse models

To generate the β-cell-specific Cisd2 KO (Cisd2 βKO) mice, Cisd2 floxed allele (Cisd2 f/f) mice were crossed with transgenic mice carrying Insulin 1-Cre (Ins1-Cre; JAX026801). From this cross Cisd2 βKO (Cisd2 f/f;Ins1-Cre) mice were obtained after two generations of breeding. All the mice used in this study are male, with a pure or congenic C57BL/6 background, and were housed under a 12-hour light–dark cycle at constant temperature of 20–22°C in a specific pathogen-free facility. Mice were euthanized using carbon dioxide (CO_2) inhalation. All animal protocols were approved by the Institutional Animal Care and Use Committee of National Yang Ming Chiao Tung University (No. 1070419) and adhered to the 3R principles (Replacement, Reduction and Refinement) according to the "Animal Protection Act" of Taiwan.

4.2. Oral glucose tolerance test, insulin tolerance test and insulin secretion assay

For the oral glucose tolerance test, mice were orally administrated a glucose solution (1.5 mg/g body weight) after fasting for 12 h (10:00 pm to 10:00 am). For the insulin tolerance test, mice were fasted for 2 h (9:00 am. to 11:00 am.) and then received an intraperitoneal injection of insulin (0.75 U/kg body weight) (Actrapid human regular insulin, Novo Nordisk, Bagsværd, Denmark). Blood samples were collected at the indicated time points. Blood glucose levels were measured using OneTouch Ultra glucose test strips and a SureStep

Brand Meter (LifeScan, Milpitas, CA, USA). Serum insulin levels were quantified using the Ultrasensitive Mouse Insulin ELISA kit (Mercodia, Uppsala, Sweden, #10-1249-01).

4.3. Molecular histopathology and transmission electron microscopy (TEM)

Mouse pancreatic tissue samples were harvested and fixed with 10% formalin for 14–16 h at 4°C. The samples were then processed using a tissue processor (STP120, MICROM, Walldorf, Germany) and embedded in paraffin. Hematoxylin and eosin (H&E) and immunohistochemistry (IHC) staining of 3–4 μm tissue sections were performed using standard protocols. The primary antibodies used were Insulin (Abcam, ab7842) and Glucagon (Sigma, G2654). TEM analysis was conducted as previously described [55]. Briefly, freshly collected mouse pancreatic tissues were fixed in TEM fixative buffer (1.5% glutaraldehyde and 1.5% paraformaldehyde in 100 mM cacodylate buffer at pH 7.3), post-fixed in 1% OsO_4 and 1.5% potassium hexanoferrate and then washed in cacodylate and 200 mM sodium maleate buffers (pH 6.0). The tissues were then block stained with 1% uranyl acetate, dehydrated, embedded in Epon (EMS, Hatfield, PA, USA, #14120) and sectioned for TEM analysis. The dilation of the ER was quantified using ImageJ software.

4.4. Isolation of the β-islets from mouse pancreas

Pancreatic β-islets were isolated from mice using a combination of enzymatic and mechanical digestion of the pancreas, which was followed by density gradient separation, as previously described [56]. The isolated β-islets were preserved in RNAlater RNA stabilization solution (Thermo, AM7020) at −20°C prior to RNA isolation.

4.5. Cell culture

The MIN6 (CRL-11506, ATCC) mouse β-cell line was maintained in the MIN6 complete medium (DMEM [11965, Gibco] supplemented with 15% fetal bovine serum, 2 mM L-glutamine, 1× penicillin and streptomycin, 1× NEAA and 9 μM β-mercaptoethanol) in a humidified incubator at 37°C with 5% CO_2. The specific treatment protocols are described in the respective figure legends.

4.6. Generation of Cisd2KO and lentivirus-mediated Cisd2 re-expression (RE) MIN6 β-cell lines

The Cisd2 gene in the MIN6 β-cell line was disrupted using the CRISPR/Cas9 system as previously described [57]. The gRNA/Cas9n (D10A) plasmids were kindly provided by Dr. Tsai-Yu Tzeng (Cancer and Immunology Research Center Genome Editing Core Facility, NYCU). These plasmids were co-transfected into MIN6 β-cells using PolyJet TM reagent (SL100688, SignaGen Laboratories). After selection of single cell colonies, Cisd2 gene deletion was confirmed by PCR and DNA sequencing. The efficiency of Cisd2 protein knockout was verified by Western blot analysis. To generate the Cisd2 re-expressed MIN6 β-cell (Cisd2RE) line, one Cisd2KO clone was subjected to lentiviral vector infection. The Cisd2 expression plasmid was packaged in lentivirus and produced by the National RNAi Core Facility at Academia Sinica in Taiwan. The Cisd2KO MIN6 β-cells were infected with the lentivirus in the presence of polybrene (8 μg/mL) in the MIN6 growth medium. After infection, cells were selected for 72 h in growth medium containing puromycin (3 μg/mL) (Invitrogen, A11138-03). The obtained stable line was maintained in complete growth medium containing a low dose of puromycin (1.5 μg/mL). The efficiency of Cisd2 re-expression was assessed by Western blot analysis.

4.7. Intracellular calcium imaging

Intracellular Ca^{2+} imaging analysis was performed as previously described [40]. Briefly, cytosolic Ca^{2+} was assayed at 37°C using a ratiometric Fura-2 fluorescence Ca^{2+} probe on a single-cell fluorimeter. MIN6 β-cells were loaded with 2 μM Fura-2/AM (Invitrogen) in culture medium at 37°C for 30 min. ER Ca^{2+} stores were depleted by treating the cells with 2 μM thapsigargin (TAG) for 9 min in Ca^{2+}-free medium. Subsequently, Ca^{2+} influx by SOCE was triggered by an exchange into extracellular Ca^{2+} medium (0–2 mM) for 5 min. Fura-2/AM were excited alternatively between 340 nm and 380 nm using a Polychrome IV monochromator (Till Photonics, Grafelfing, Germany). Images were captured using an Olympus IX71 inverted microscope equipped with a xenon illumination system and an IMAGO CCD camera (Till Photonics). The intensity of fluorescence emission at 510 nm was recorded, stored digitally, and analyzed using the program TILLvisION 4.0 (Till Photonics, Grafelfing, Germany). Specific treatment protocols are detailed in the corresponding figures and legends.

4.8. Measurement of the mitochondrial oxygen consumption rate by the MIN6 β-cell line

The mitochondrial oxygen consumption rate (OCR) was measured using a XF^e24 analyzer (Seahorse Bioscience, North Billerica, MA, USA) as previously described [12]. Briefly, MIN6 cells (4×10^3 cells/well) were seeded onto a XF24 V7 plate and cultured in MIN6 complete growth medium for 12–16 h. The culture medium was then replaced with fresh assay medium (sodium bicarbonate free DMEM [Sigma, D5648] supplemented with 2% FBS, 2 mM glutamine, 100 U/ml penicillin, 100 μg/mL streptomycin and 1% NEAA) for 1 h prior to OCR measurement. OCR was measured at 37°C before and after sequential addition of the following compounds: 1 μM oligomycin A (an ATP synthase inhibitor), 3 μM FCCP (a potent uncoupler of oxidative phosphorylation), and 1 μM rotenone (a mitochondrial complex I inhibitor) with 1 μM antimycin A (a mitochondrial complex III inhibitor). This procedure enabled the assessment of OCR contributions from mitochondrial basal respiration, ATP-linked respiration, maximum respiration, and non-mitochondrial respiration [58]. Results are presented in pmol/minute/μg protein.

4.9. Western blotting

Cell samples were homogenized in the RIPA lysis buffer (50 mM Tris at pH 7.4, 150 mM NaCl, 0.5% Sodium deoxycholate, 0.1% SDS and 1% Triton X-100) supplemented with complete protease inhibitor and phosphatase inhibitor cocktails (Roche). The samples were then denatured in SDS sample buffer (50 mM Tris at pH 6.8, 100 mM dithiothreitol, 2% SDS and 10% glycerol) for 10 min at 100°C. The extracted proteins were separated by SDS-polyacrylamide gel electrophoresis (Bio-Rad, Hercules, CA, USA) and then electro-transferred to a polyvinylidene fluoride membrane (PerkinElmer, Waltham, MA, USA). Next, the membranes were blocked with 5% (w/v) non-fat dried milk solution for 1 h at room temperature, which was followed by incubation with each of the specific primary antibodies for 16 h at 4°C. The membranes were then washed, which was followed by incubation with the relevant secondary antibodies. Protein signals were detected using a visualizer kit (Millipore, Burlington, MA, USA, WBKLS0500). The following antibodies were used: Cisd2 [12], Gapdh (Millipore, MAB374), β-tubulin (Millipore, 05661), eIF2α (Cell signaling, 9722), p-eIF2α (Cell signaling, 3398), Calnexin (Sigma, C4731), Vdac1 (Millipore, MABN504), Anti-Rabbit IgG HRP Linked (Sigma, NA934) and Anti-Mouse IgG HRP Linked (Sigma, NA931).

4.10. Real-time RT-qPCR

Total RNA was extracted from MIN6 cells using TRI Reagent (Sigma—Aldrich, T9424). The cDNA was synthesized from total RNA by reverse transcription using random hexamers (Roche, 11034731001) and SuperScript™ III reverse transcriptase (Invitrogen, 18080) according to the manufacturer's instructions. Real-time quantitative PCR was then performed using the synthesized cDNA.

4.11. RNA isolation for RNA sequencing, and pathway analysis

Total RNA was isolated from RNAlater-preserved mouse β-islets using an RNA extraction kit (Thermo, 12183018A). RNA sequencing and pathway analyses were conducted as previously described [59]. Briefly, RNA sequencing was performed by Genomics Center for Clinical and Biotechnological Applications, National Yang Ming Chiao Tung University using single-end sequencing with a depth of at least 20 million reads per sample. After mapping, unique gene reads were analyzed as expected counts in order to assess gene expression. A total of 8,616 genes were analyzed after filtering to identify genes expressed in mouse β-islets (minimal expected counts >200 detected in at least 50% of samples). Normalized counts and the differentially expressed genes (DEGs) were obtained using DESeq2 (using the Wald test), with a false discovery rate (FDR) controlled to be below 0.05. Enrichment analyses of Gene Ontology (GO) biological process annotations and KEGG pathway analysis were conducted using the online tool STRING (https://string-db.org). Canonical pathway analysis and upstream analysis were performed using QIAGEN Ingenuity Pathway Analysis (IPA) software (Ingenuity Systems®, www.ingenuity.com). The normalized counts were transformed into z-scores (normalized counts minus mean and divided by standard deviation [SD]) and these z-scores were used to generate heatmaps using Multi Experiment Viewer 4.9 software (mev.tm4.org).

4.12. Statistical analysis

Data are presented as mean ± standard deviation (SD) or mean ± standard error of the mean (SEM) as indicated in the figure legends. Comparisons between two groups were performed using unpaired two-tailed Student's t tests. Comparisons among multiple groups were conducted using one-way ANOVA with the Bonferroni multiple comparison test. Statistical significance was defined as $p < 0.05$. All statistical analyses were conducted using GraphPad Prism software (v10.0, GraphPad Software, San Diego, CA, USA).

ACKNOWLEDGMENTS

We thank Chia-Sheng Cheng, Yao-Kuan Huang, Tai-Wen Wang and Yuan-Chi Teng for their technical assistance. The authors acknowledge the sequencing and bioinformatic services provided by the National Genomics Center for Clinical and Biotechnological Applications of the Cancer and Immunology Research Center at National Yang Ming Chiao Tung University and the National Core Facility for Biopharmaceuticals (NCFB) of the National Science and Technology Council. We also thank the following core facilities: (1) Imaging Core Facility of National Yang Ming Chiao Tung University for imaging service; (2) Microscopy Center at Chang Gung University for the TEM service; (3) National RNAi Core Facility at Academia Sinica in Taiwan for the shRNA service; (4) The Bioimage Core Facility of the National Core Facility for Biopharmaceuticals in Taiwan for technical services. We also acknowledge support by the Interdisciplinary Research Center for Healthy Longevity of National Yang Ming Chiao Tung University from the Featured Areas Research Center Program within the framework of the Higher Education Sprout Project by the Ministry of Education (MOE) in Taiwan.

CRediT AUTHORSHIP CONTRIBUTION STATEMENT

Zhao-Qing Shen: Writing — original draft, Validation, Methodology, Investigation, Formal analysis, Data curation, Conceptualization. **Wen-Tai Chiu:** Writing — original draft, Validation, Methodology, Investigation, Formal analysis, Data curation, Conceptualization. **Cheng-Heng Kao:** Writing — original draft, Validation, Methodology, Investigation, Formal analysis, Data curation. **Yu-Chen Chen:** Methodology, Investigation, Data curation. **Li-Hsien Chen:** Validation, Methodology, Formal analysis, Data curation. **Tsai-Wen Teng:** Methodology, Formal analysis, Data curation. **Shao-Yu Hsiung:** Methodology, Data curation. **Tsai-Yu Tzeng:** Methodology, Investigation. **Chien-Yi Tung:** Validation, Methodology, Data curation. **Chi-Chang Juan:** Supervision, Investigation. **Ting-Fen Tsai:** Writing — review & editing, Visualization, Validation, Project administration, Investigation, Funding acquisition, Formal analysis, Conceptualization.

DECLARATION OF COMPETING INTEREST

The authors declare that they have no known competing financial interests or personal relationships that could have appeared to influence the work reported in this paper.

FUNDING SOURCES

The work was supported by grants from the National Science and Technology Council (MOST 107-2320-B-010-037-MY3 to TFT) and from the National Health Research Institutes (NHRI-11A1-CG-CO-07-2225-1, NHRI-12A1-CG-CO-07-2225-1 and NHRI-13A1-CG-CO-07-2225-1 to TFT).

DATA AVAILABILITY

Data will be made available on request.

APPENDIX A. SUPPLEMENTARY DATA

Supplementary data to this article can be found online at https://doi.org/10.1016/j.molmet.2025.102140.

REFERENCES

[1] Fischer TT, Ehrlich BE. Wolfram syndrome: a monogenic model to study diabetes mellitus and neurodegeneration. Curr Opin Physiol 2020;17:115—23.
[2] Stone SI, Balasubramanyam A, Posey JE. Atypical diabetes: what have we learned and what does the future hold? Diabetes Care 2024;47(5):770—81.
[3] Tamaroff J, Kilberg M, Pinney SE, McCormack S. Overview of atypical diabetes. Endocrinol Metabol Clin 2020;49(4):695—723.
[4] Loncke J, Vervliet T, Parys JB, Kaasik A, Bultynck G. Uniting the divergent wolfram syndrome-linked proteins WFS1 and CISD2 as modulators. Sci Signal 2021;14:eabc6165.
[5] Tokarz VL, MacDonald PE, Klip A. The cell biology of systemic insulin function. J Cell Biol 2018;217(7):2273—89.
[6] Zhang IX, Raghavan M, Satin LS. The endoplasmic reticulum and calcium homeostasis in pancreatic beta cells. Endocrinology 2020;161(2).

[7] Chen YF, Kao CH, Chen YT, Wang CH, Wu CY, Tsai CY, et al. Cisd2 deficiency drives premature aging and causes mitochondria-mediated defects in mice. Genes Dev 2009;23(10):1183–94.
[8] Wiley SE, Andreyev AY, Divakaruni AS, Karisch R, Perkins G, Wall EA, et al. Wolfram syndrome protein, Miner1, regulates sulphydryl redox status, the unfolded protein response, and Ca^{2+} homeostasis. EMBO Mol Med 2013;5(6):904–18.
[9] Shen ZQ, Huang YL, Teng YC, Wang TW, Kao CH, Yeh CH, et al. CISD2 maintains cellular homeostasis. Biochim Biophys Acta Mol Cell Res 2021;1868(4):118954.
[10] Chen YF, Wu CY, Kirby R, Kao CH, Tsai TF. A role for the CISD2 gene in lifespan control and human disease. Ann N Y Acad Sci 2010;1201:58–64.
[11] Yeh CH, Shen ZQ, Lin CC, Lu CK, Tsai TF. Rejuvenation: turning back time by enhancing CISD2. Int J Mol Sci 2022;23(22).
[12] Shen ZQ, Chen YF, Chen JR, Jou YS, Wu PC, Kao CH, et al. CISD2 haploinsufficiency disrupts calcium homeostasis, causes nonalcoholic fatty liver disease, and promotes hepatocellular carcinoma. Cell Rep 2017;21(8):2198–211.
[13] Yeh CH, Shen ZQ, Hsiung SY, Wu PC, Teng YC, Chou YJ, et al. Cisd2 is essential to delaying cardiac aging and to maintaining heart functions. PLoS Biol 2019;17(10):e3000508.
[14] Tong X, Kono T, Anderson-Baucum EK, Yamamoto W, Gilon P, Lebeche D, et al. SERCA2 deficiency impairs pancreatic beta-cell function in response to diet-induced obesity. Diabetes 2016;65(10):3039–52.
[15] Iida H, Kono T, Lee CC, Krishnan P, Arvin MC, Weaver SA, et al. SERCA2 regulates proinsulin processing and processing enzyme maturation in pancreatic beta cells. Diabetologia 2023;66(11):2042–61.
[16] Campbell JE, Newgard CB. Mechanisms controlling pancreatic islet cell function in insulin secretion. Nat Rev Mol Cell Biol 2021;22(2):142–58.
[17] Seino S, Shibasaki T, Minami K. Dynamics of insulin secretion and the clinical implications for obesity and diabetes. J Clin Investig 2011;121(6):2118–25.
[18] Tuduri E, Soriano S, Almagro L, Montanya E, Alonso-Magdalena P, Nadal Á, et al. The pancreatic beta-cell in ageing: implications in age-related diabetes. Ageing Res Rev 2022;80:101674.
[19] Liu M, Huang Y, Xu X, Li X, Alam M, Arunagiri A, et al. Normal and defective pathways in biogenesis and maintenance of the insulin storage pool. J Clin Investig 2021;131(2).
[20] Sun CC, Lee SY, Chen LH, Lai CH, Shen ZQ, Chen NN, et al. Targeting Ca^{2+}-dependent pathways to promote corneal epithelial wound healing induced by CISD2 deficiency. Cell Signal 2023;109:110755.
[21] Skelin M, Rupnik M, Cencič A. Pancreatic beta cell lines and their applications in diabetes mellitus research. ALTEX-Alternatives to animal experimentation 2010;27:105–13.
[22] Meyerovich K, Ortis F, Cardozo AK. The non-canonical NF-kappaB pathway and its contribution to beta-cell failure in diabetes. J Mol Endocrinol 2018;61(2):F1–6.
[23] Li X, Wu Y, Song Y, Ding N, Lu M, Jia L, et al. Activation of NF-kappaB-Inducing kinase in islet beta cells causes beta cell failure and diabetes. Mol Ther 2020;28(11):2430–41.
[24] Baumel-Alterzon S, Katz LS, Brill G, Garcia-Ocana A, Scott DK. Nrf2: the master and captain of beta cell fate. Trends Endocrinol Metabol 2021;32(1):7–19.
[25] Cheng Y, Niu Z, Cai Y, Zhang W. Emerging role of UFMylation in secretory cells involved in the endocrine system by maintaining ER proteostasis. Front Endocrinol 2022;13:1085408.
[26] Chen H, Gu X, Liu Y, Wang J, Wirt SE, Bottino R, et al. PDGF signalling controls age-dependent proliferation in pancreatic beta-cells. Nature 2011;478(7369):349–55.
[27] Li Y, Wang X, Yang B, Wang H, Ma Z, Lu Z, et al. 3beta-Hydroxysteroid-Delta24 reductase (DHCR24) protects pancreatic beta cells from endoplasmic reticulum stress-induced apoptosis by scavenging excessive intracellular reactive oxygen species. J Diabetes Res 2020;2020:3426902.
[28] Maachi H, Fergusson G, Ethier M, Brill GN, Katz LS, Honig LB, et al. HB-EGF signaling is required for glucose-induced pancreatic beta-cell proliferation in rats. Diabetes 2020;69(3):369–80.
[29] Barsby T, Otonkoski T. Maturation of beta cells: lessons from in vivo and in vitro models. Diabetologia 2022;65(6):917–30.
[30] Liang R, Liu N, Cao J, Liu T, Sun P, Cai X, et al. HIF-1alpha/FOXO1 axis regulated autophagy is protective for beta cell survival under hypoxia in human islets. Biochim Biophys Acta, Mol Basis Dis 2022;1868(5):166356.
[31] Wen X, Yang Y. Emerging roles of GLIS3 in neonatal diabetes, type 1 and type 2 diabetes. J Mol Endocrinol 2017;58(2):R73–85.
[32] Low BSJ, Lim CS, Ding SSL, Tan YS, Ng NHJ, Krishnan VG, et al. Decreased GLUT2 and glucose uptake contribute to insulin secretion defects in MODY3/HNF1A hiPSC-derived mutant beta cells. Nat Commun 2021;12(1):3133.
[33] Miyachi Y, Miyazawa T, Ogawa Y. HNF1A mutations and beta cell dysfunction in diabetes. Int J Mol Sci 2022;23(6).
[34] Robertson CC, Elgamal RM, Henry-Kanarek BA, Arvan P, Chen S, Dhawan S, et al. Untangling the genetics of beta cell dysfunction and death in type 1 diabetes. Mol Metabol 2024;86:101973.
[35] Moin ASM, Butler AE. Alterations in beta cell identity in type 1 and type 2 diabetes. Curr Diabetes Rep 2019;19(9):83.
[36] Sun B, Chen H, Xue J, Li P, Fu X. The role of GLUT2 in glucose metabolism in multiple organs and tissues. Mol Biol Rep 2023;50(8):6963–74.
[37] Samadli S, Zhou Q, Zheng B, Gu W, Zhang A. From glucose sensing to exocytosis: takes from maturity onset diabetes of the young. Front Endocrinol 2023;14:1188301.
[38] Wang CH, Chen YF, Wu CY, Wu PC, Huang YL, Kao CH, et al. Cisd2 modulates the differentiation and functioning of adipocytes by regulating intracellular Ca^{2+} homeostasis. Hum Mol Genet 2014;23(18):4770–85.
[39] Rouzier C, Moore D, Delorme C, Lacas-Gervais S, Ait-El-Mkadem S, Fragaki K, et al. A novel CISD2 mutation associated with a classical Wolfram syndrome phenotype alters Ca^{2+} homeostasis and ER-mitochondria interactions. Hum Mol Genet 2017;26(9):1599–611.
[40] Sun CC, Lee SY, Kao CH, Chen LH, Shen ZQ, Lai CH, et al. Cisd2 plays an essential role in corneal epithelial regeneration. EBioMedicine 2021;73:103654.
[41] Choi UY, Choi YJ, Lee SA, Yoo JS. Cisd2 deficiency impairs neutrophil function by regulating calcium homeostasis via Calnexin and SERCA. BMB Rep 2024;57(5):256–61.
[42] Liiv M, Vaarmann A, Safiulina D, Choubey V, Gupta R, Kuum M, et al. ER calcium depletion as a key driver for impaired ER-to-mitochondria calcium transfer and mitochondrial dysfunction in Wolfram syndrome. Nat Commun 2024;15(1):6143.
[43] Lu S, Kanekura K, Hara T, Mahadevan J, Spears LD, Oslowski CM, et al. A calcium-dependent protease as a potential therapeutic target for Wolfram syndrome. Proc Natl Acad Sci U S A 2014;111(49):E5292–301.
[44] Abreu D, Asada R, Revilla JMP, Lavagnino Z, Kries K, Piston DW, et al. Wolfram syndrome 1 gene regulates pathways maintaining beta-cell health and survival. Lab Invest 2020;100(6):849–62.
[45] Abreu D, Urano F. Current landscape of treatments for Wolfram syndrome. Trends Pharmacol Sci 2019;40(10):711–4.
[46] Mishra R, Chen BS, Richa P, Yu-Wai-Man P. Wolfram syndrome: new pathophysiological insights and therapeutic strategies. Ther Adv Respir Dis 2021;2:26330040211039518.
[47] Zarain-Herzberg A, Garcia-Rivas G, Estrada-Aviles R. Regulation of SERCA pumps expression in diabetes. Cell Calcium 2014;56(5):302–10.
[48] Kong L, Zhao Q, Jiang X, Hu J, Jiang Q, Sheng L, et al. Trimethylamine N-oxide impairs beta-cell function and glucose tolerance. Nat Commun 2024;15(1):2526.

[49] Nguyen HT, Noriega Polo C, Wiederkehr A, Wollheim CB, Park KS. CDN1163, an activator of sarco/endoplasmic reticulum Ca^{2+} ATPase, up-regulates mitochondrial functions and protects against lipotoxicity in pancreatic beta-cells. Br J Pharmacol 2023;180(21):2762—76.
[50] Danielpur L, Sohn YS, Karmi O, Fogel C, Zinger A, Abu-Libdeh A, et al. GLP-1-RA corrects mitochondrial labile iron accumulation and improves beta-cell function in type 2 Wolfram syndrome. J Clin Endocrinol Metab 2016;101(10):3592—9.
[51] Viskupicova J, Rezbarikova P. Natural polyphenols as SERCA activators: role in the endoplasmic reticulum stress-related diseases. Molecules 2022;27(16).
[52] Leiter EH. The genetics of diabetes susceptibility in mice. FASEB J 1989;3:2231—41.
[53] Morikawa S, Tanabe K, Kaneko N, Hishimura N, Nakamura A. Comprehensive overview of disease models for Wolfram syndrome: toward effective treatments. Mamm Genome 2024;35(1):1—12.
[54] Maxwell KG, Millman JR. Applications of iPSC-derived beta cells from patients with diabetes. Cell Reports Medicine 2021;2(4):100238.
[55] Yeh CH, Shen ZQ, Wang TW, Kao CH, Teng YC, Yeh TK, et al. Hesperetin promotes longevity and delays aging via activation of Cisd2 in naturally aged mice. J Biomed Sci 2022;29(1):53.
[56] Graham KL, Fynch S, Pappas EG, Tan C, Kay TW, Thomas HE. Isolation and culture of the islets of Langerhans from mouse pancreas. Bio-protocol 2016;6(12):e1840.
[57] Huang YL, Shen ZQ, Huang CH, Lin CH, Tsai TF. Cisd2 slows down liver aging and attenuates age-related metabolic dysfunction in male mice. Aging Cell 2021;20(12):e13523.
[58] Gu X, Ma Y, Liu Y, Wan Q. Measurement of mitochondrial respiration in adherent cells by seahorse XF96 cell mito stress test. STAR Protoc 2021;2(1):100245.
[59] Shen ZQ, Chang CY, Yeh CH, Lu CK, Hung HC, Wang TW, et al. Hesperetin activates CISD2 to attenuate senescence in human keratinocytes from an older person and rejuvenates naturally aged skin in mice. J Biomed Sci 2024;31(1):15.

